Cell Metabolism, Volume *18*

Supplemental Information

Reciprocal Regulation of Hepatic and Adipose Lipogenesis by Liver X Receptors in Obesity and Insulin Resistance

Simon W. Beaven, Aleksey Matveyenko, Kevin Wroblewski, Lily Chao, Damien Wilpitz, Tu Wen Hsu, Jacob Lentz, Brian Drew, Andrea L. Hevener, and Peter Tontonoz

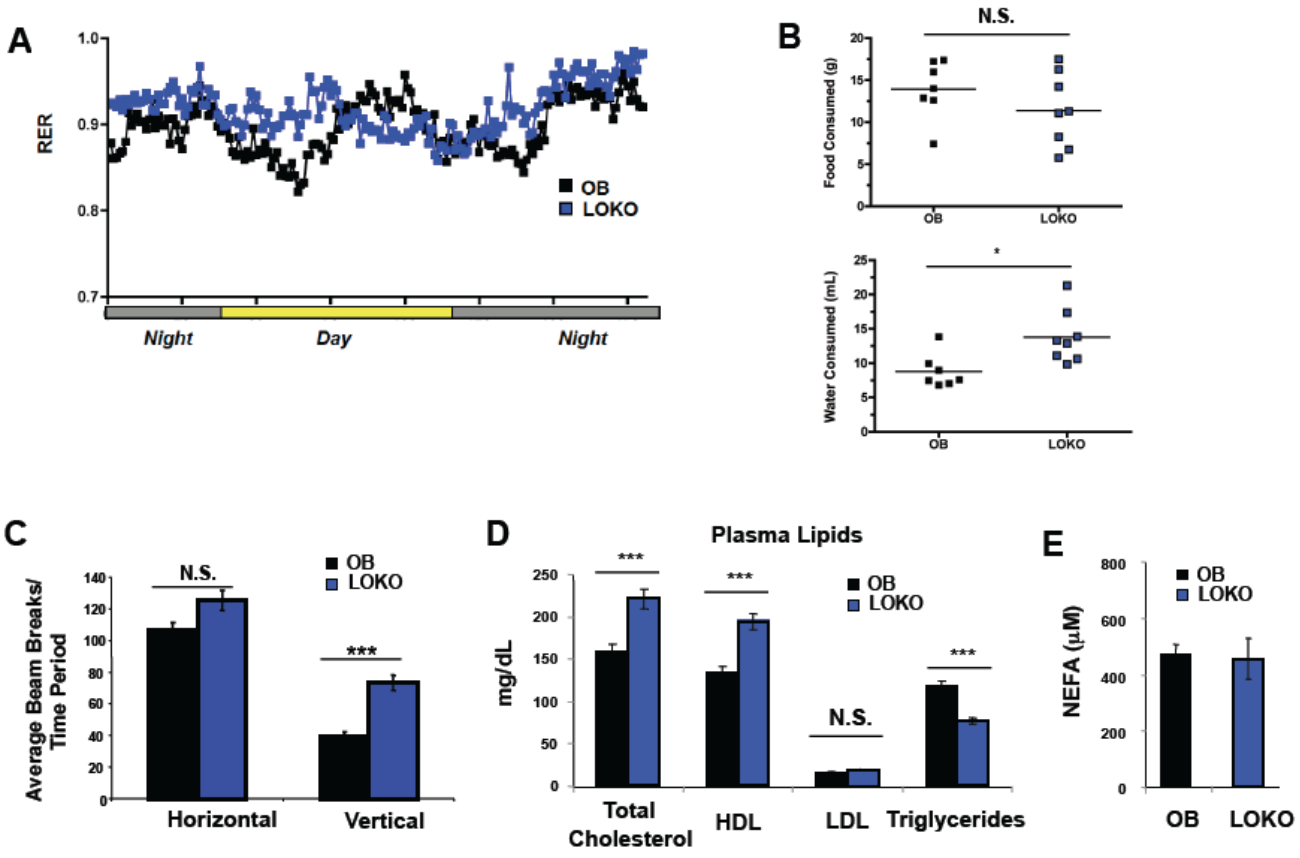

Figure S1. **Indirect Calorimetry and Lipid Analysis of LOKO Mice, Related to Figure 1**

(A) Indirect calorimetry was performed as described in Methods. Data were collected every 20 minutes across a full day / night period and the RER is plotted. **(B)** Food consumption and water

volume delivered was tracked during indirect calorimetry. **(C)** Beam breaks in both the horizontal and vertical planes are expressed as the average number of beam breaks per time period. **(D & E)** Quantitative plasma cholesterol, triglyceride, and non-esterified free fatty acid (NEFA) levels from OB and LOKO mice. Statistical analysis by 2-way ANOVA **(A)** or Student's t-test **(B-E)** with Bonferroni post-tests: *, P < 0.05; ***, P < 0.001; N.S. not significant.

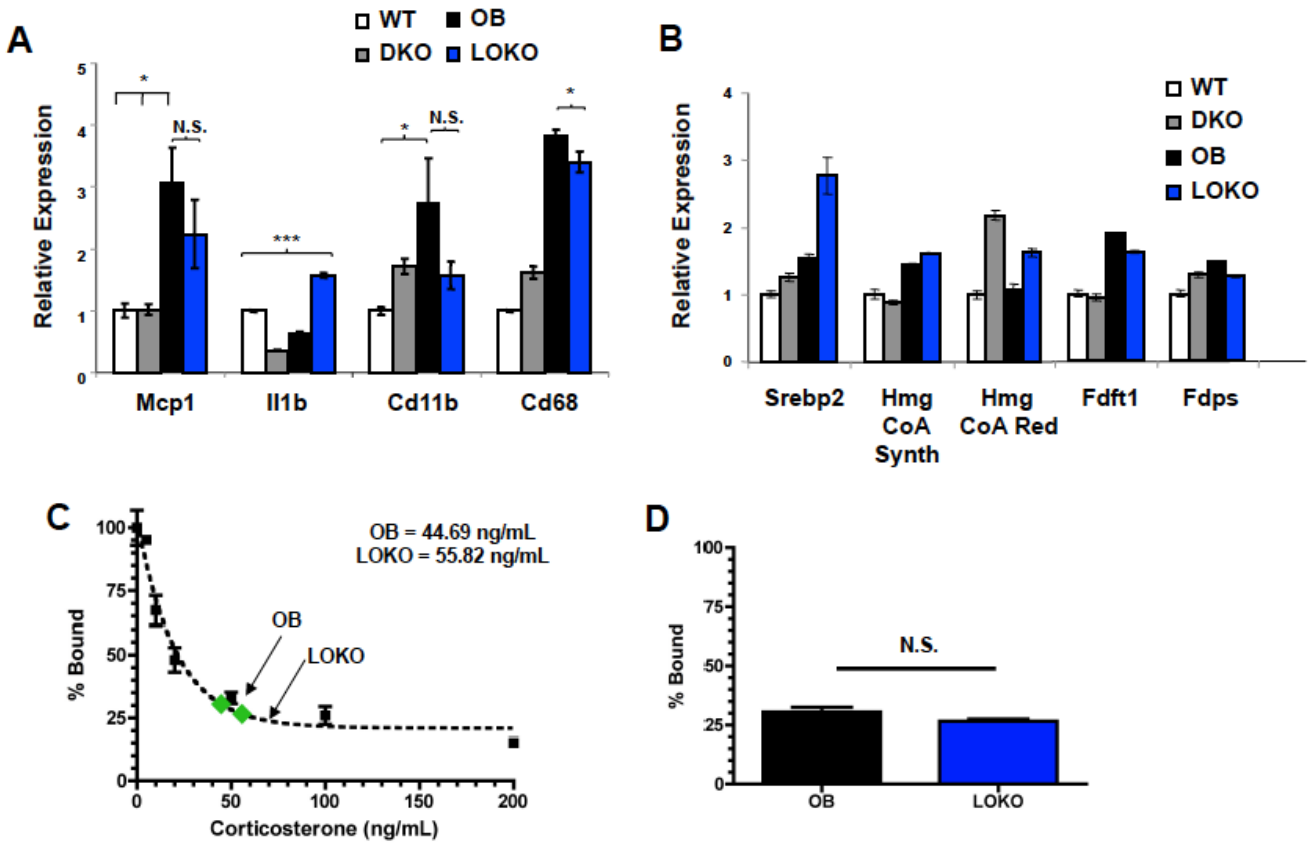

Figure S2. Hepatic Gene Expression and Glucocorticoid Levels in LOKO Mice, Related to Figure 2

Additional gene expression for **(A)** inflammatory and macrophage markers and **(B)** *Srebp2* and some if its target genes from the livers of WT, DKO, OB, and LOKO mice (N = 5-9 mice per group) at 24 weeks of age. Results were normalized first to expression of the housekeeping gene 36B4 and shown as fold induction over WT animals. Values are means +/- SEM. Statistical analysis by 1-way

ANOVA with Bonferroni post-tests: *, P < 0.05; ***, P < 0.001, N.S. not significant. (**C,D**) Corticosterone levels were determined from the plasma of OB and LOKO mice by a tritiated (^{3}H) radio-immune assay according to the manufacturer's protocol (MP Biomedical). A standard curve for bound tritium in relation to corticosterone concentration is shown (C) with the percent bound levels from five OB and LOKO mice shown along with the calculated concentrations from each genotype (D). Statistical analysis by Student's t-test: N.S. not significant.

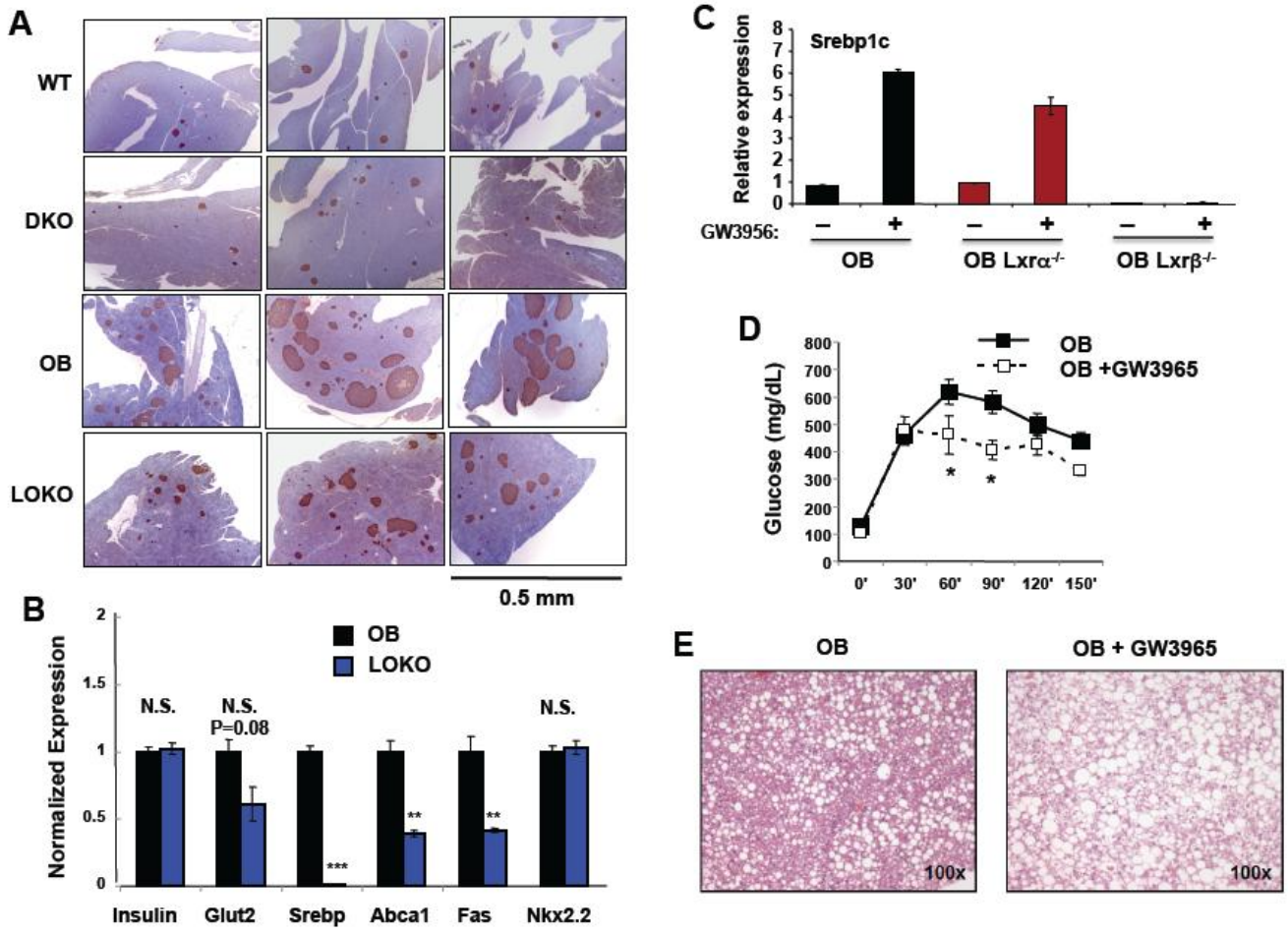

Figure S3. LOKO Mice Have Decreased β Cell Mass, Related to Figure 3

(A) Representative pancreatic sections, 3 from each of the WT, DKO, OB, and LOKO genotypes are shown, immunostained for insulin (brown). **(B)** Pancreatic islets were isolated from OB and LOKO

mice (n=4 per group) as described in Methods. RNA was immediately extracted (*ex vivo*) for gene expression analysis by real-time PCR. **(C)** The LXR ligand, GW3965 (1 μM), induces *Srebp1c* only in primary pancreatic islets from obese mice with *Lxrβ* [OB and OB *Lxrα*$^{-/-}$], demonstrating that Lxrβ is the predominant, functional LXR in the pancreas. **(D)** OB mice were fed a diet containing the LXR ligand GW3965 (0.012%) for 10 days. The results of an intraperitoneal glucose tolerance test are shown. Experiment performed twice with comparable results. **(E)** LXR agonist worsens the steatosis of OB mice. Magnification 100x. Values are expressed as means +/- SEM. Statistical analysis by Student's t-test: **, P < 0.01; ***, P < 0.001; N.S. not significant.

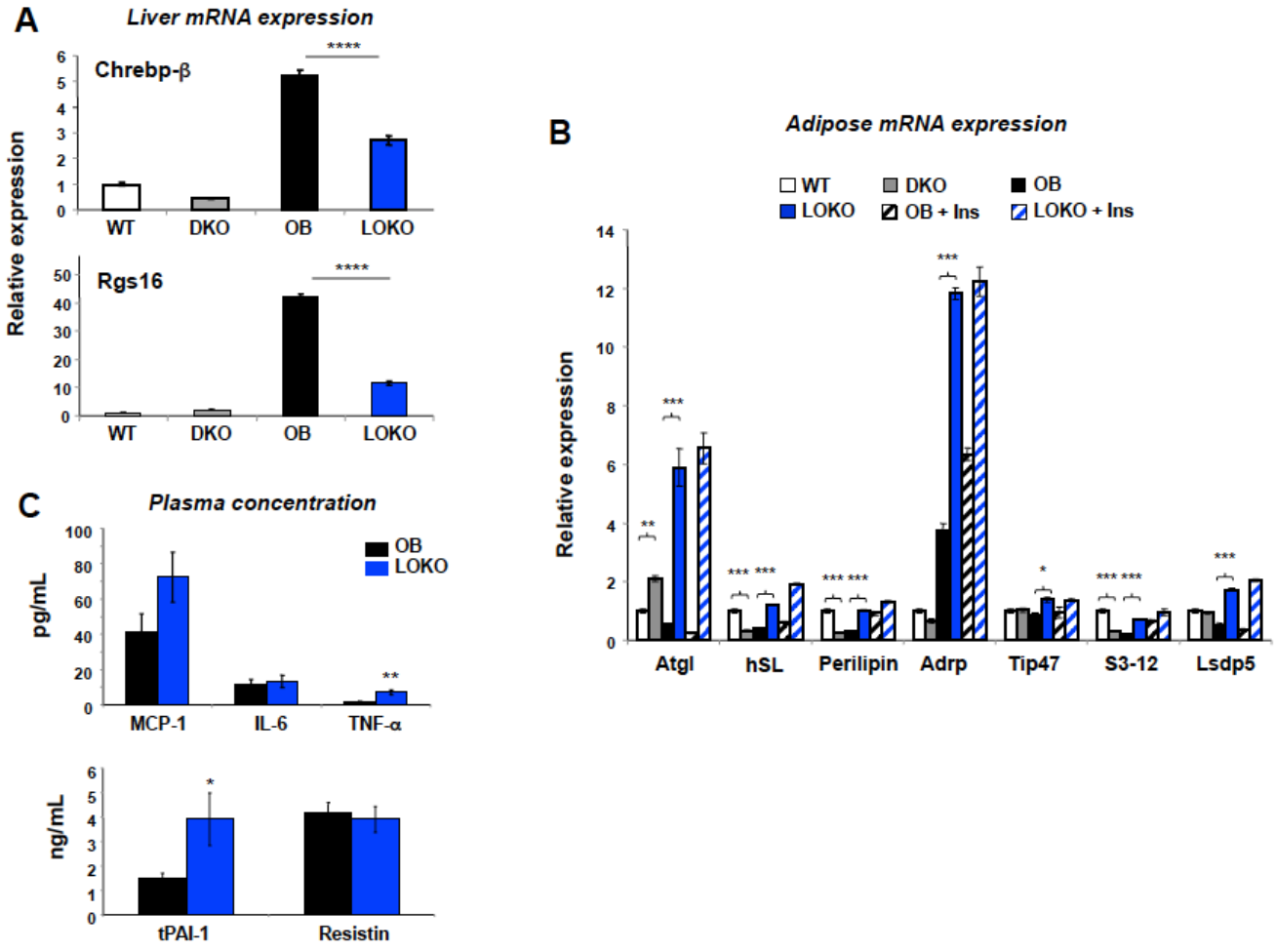

Figure S4. Tissue-Specific Regulation of ChREBP Expression in LOKO Mice, Related to Figure 4

(A) Real-time PCR analysis of *Chrebp*-β and its target gene *Rgs*16 gene expression in liver shows a reciprocal decrease specifically in LOKO livers (compare to Fig 4E). **(B)** Gene expression analysis of adipose tissue lipases and lipid droplet perilipin gene family in adipose tissue. **(C)** Analysis of inflammatory cytokines in plasma from OB and LOKO mice using a multiplexed bead assay (Luminex, Millipore). Values are means +/- S.E.M. Statistical analysis by Student's t-test: *, $P < 0.05$; **, $P < 0.01$; ***, $P < 0.001$.